Blombäck, B., Hessel, B., Hogg, D., & Therkildsen, L. (1978) *Nature (London) 257*, 501.
Calvert, P. D., Nichol, L. W., & Sawyer, W. H. (1979) *J. Theor. Biol. 80*, 223.
Chavez, L. G., Jr., & Scheraga, H. A. (1980) *Biochemistry 19*, 1005.
Chung, D. W., Rixon, M. W., MacGilivray, R. T. A., & Davie, E. W. (1981) *Proc. Natl. Acad. Sci. U.S.A. 78*, 1466.
Ciernewski, C. S., & Edgington, T. S. (1979) *Thromb. Res. 14*, 747.
Doolittle, R. F., & Blombäck, B. (1964) *Nature (London) 202*, 147.
Eckhardt, T., Nossel, H. L., Hurlet-Jensen, A., LaGamma, K. S., Owen, J., & Auerbach, M. (1981) *J. Clin. Invest. 67*, 809.
Feldman, H., & Rodbard, D. (1971) in *Principles of Competitive Protein-Binding Assays* (Odell, W. D., & Daughaday, W. H., Eds.) p 158, Lippincott, Philadelphia, PA.
Hageman, T. C., & Scheraga, H. A. (1974) *Arch. Biochem. Biophys. 164*, 707.
Hageman, T. C., & Scheraga, H. A. (1977) *Arch. Biochem. Biophys. 179*, 506.
Hanna, L. S., Scheraga, H. A., Francis, C. W., & Marder, V. J. (1984) *Biochemistry 23*, 4681–4687.
Hessel, B., Makino, M., Iwanaga, S., & Blombäck, B. (1979) *Eur. J. Biochem. 98*, 521.
Higgins, D. L., Lewis, S. D., & Shaffer, J. A. (1983) *J. Biol. Chem. 258*, 9276.
Hurlet-Jensen, A., Cummins, H. Z., Nossel, H. L., & Liu, C. Y. (1982) *Thromb. Res. 27*, 419.
Iwanaga, S., Wallen, P., Grondahl, N. J., Henschen, A., & Blombäck, B. (1969) *Eur. J. Biochem. 8*, 189.
Kudryk, B., Reuterby, J., & Blombäck, B. (1974) *Eur. J. Biochem. 46*, 141.
Kudryk, B., Robinson, D., Netrē, C., Hessel, B., Blombäck, M., & Blombäck, B. (1982) *Thromb. Res. 25*, 277.
Kudryk, B., Rohoza, A., Ahadi, Z., Chin, J., & Wiebe, M. (1983) *Mol. Immunol. 20*, 1191.
Marsh, H. C., Jr., Meinwald, Y. C., Thannhauser, T. W., & Scheraga, H. A. (1983) *Biochemistry 22*, 4170.
Martinelli, R. A., & Scheraga, H. A. (1979) *Anal. Biochem. 96*, 246.
Martinelli, R. A., & Scheraga, H. A. (1980) *Biochemistry 19*, 2343.
Martinelli, R. A., Inglis, A. S., Rubira, M. R., Hageman, T. C., Hurrell, J. G. R., Leach, S. J., & Scheraga, H. A. (1979) *Arch. Biochem. Biophys. 192*, 27.
Nagy, J. A., Meinwald, Y. C., & Scheraga, H. A. (1982) *Biochemistry 21*, 1794.
Nichol, L. W., & Winzor, D. J. (1976) *Biochemistry 15*, 3015.
Plow, E. F., & Edgington, T. S. (1982) *Semin. Thromb. and Hemostasis 8*, 36.
Rodbard, D., & Hutt, D. M. (1974) in *Radioimmunoassay and Related Procedures in Medicine*, Vol. 1, p 165, International Atomic Energy Agency, Vienna.
Sachs, D. H., Schechter, A. N., Eastlake, A., & Anfinsen, C. B. (1972) *Proc. Natl. Acad. Sci. U.S.A. 69*, 3790.
Scatchard, G. (1949) *Ann. N.Y. Acad. Sci. 51*, 660.
Tanswell, P., Stan-Lotter, H., Gollwitzer, R., & Timpl, R. (1977) *Immunochemistry 14*, 277.
Timpl, R., Fietzek, P. P., Wachter, E., & Van Delden, V. (1977) *Biochim. Biophys. Acta 490*, 420.
Watt, K. W. K., Takagi, T., & Doolittle, R. F. (1978) *Proc. Natl. Acad. Sci. U.S.A. 75*, 1731.

Phosphorus-31 Nuclear Magnetic Resonance of Highly Oriented DNA Fibers. 1. Static Geometry of DNA Double Helices†

H. Shindo,*,‡ T. Fujiwara,§ H. Akutsu,§ U. Matsumoto,‡ and Y. Kyogoku§

Tokyo College of Pharmacy, Hachioji, Tokyo 192-03, Japan, and Institute for Protein Research, Osaka University, Suita 565, Japan

Received June 18, 1984

ABSTRACT: The static geometry of the phosphodiesters in oriented fibers of DNA and a variety of polynucleotides was investigated by solid-state ^{31}P nuclear magnetic resonance (NMR) spectroscopy. The structural parameters of the phosphodiester backbone expressed by two Euler angles β and γ were estimated on the basis of the NMR spectra of natural DNA, poly(dA)·poly(dT), poly(rA)·poly(dT), and poly(rA)·poly(rU). The Euler angles were calculated by using the known single crystal structures of a decamer, r(GCG)d(TATACGC), and a dodecamer, d(CGCGAATTCGCG). The distribution pattern of the Euler angles was quite different between these two oligonucleotides due to the different types of conformation, and it was fully consistent with the ^{31}P NMR results, showing that the conformation of the B form DNA is very heterogeneous while that of the A or A′ form is much more invariable with regard to the base composition. The structural parameters were also calculated by using various structures determined by the X-ray fiber diffraction studies, and they were evaluated on the basis of the ^{31}P NMR data. Notably, poly(dA)·poly(dT) fibers exhibited abnormal ^{31}P NMR spectra which were very broad in line width and were not appreciably perturbed by hydration; a coiled double-helical structure is proposed as the most plausible model for this polymer.

The polymorphism of the helical structures of deoxyribonucleic acid (DNA)[1] and synthetic polynucleotides has long been investigated mainly by the X-ray fiber diffraction method (Leslie et al., 1980, and references therein) and recently by

† Supported by a Grant-in-Aid for Scientific Research (56470132).
‡ Tokyo College of Pharmacy.
§ Institute for Protein Research.

[1] Abbreviations: NMR, nuclear magnetic resonance; DNA, deoxyribonucleic acid; RNA, ribonucleic acid; RH, relative humidity; EDTA, ethylenediaminetetraacetate; DNase, deoxyribonuclease.

0006-2960/85/0424-0887$01.50/0

a variety of other methods [see the review of Zimmerman (1982), and references therein]. However, it is often asked whether the three-dimensional structures of DNA determined for its crystalline forms are the same as those in solution. Particularly for DNA fibers, various crystal packing forces and hydration of water molecules are known to cause conformational changes such as a transition from the A to B form DNA (Cooper & Hamilton, 1966). In order to emphasize the base sequence dependence of the secondary structures, it is, therefore, desirable to study the structure of DNA under the hydrated conditions or in the solution-like state where intermolecular interactions may be weakened or negligible. Because of the shortage in number of X-ray diffractions and also of the diffused diffraction spots from the hydrated form of DNA fibers, detailed local conformations could not be detected by the X-ray method. Thus, the average single conformation has usually been assumed for the hydrated form (i.e., the B form) of DNA irrespective of the base composition.

Recently, the first skepticism about this assumption has stemmed from the DNase digestion study as well as from the X-ray diffraction studies with poly(dA-dT)·poly(dA·dT) and led to the "alternating B form of DNA" for the structure of DNA with alternating base sequence (Klug et al., 1979). Direct evidence for this has emerged from the ^{31}P NMR studies of poly(dA-dT)·poly(dA-dT) (Shindo et al., 1979) and others (Patel et al., 1979; Cohen et al., 1981; Eckstein & Jovin, 1983; McIntosh et al., 1983). These and other ^{31}P NMR studies of oriented DNA fibers (Shindo & Zimmerman, 1980), therefore, provided the evidence that natural DNA under hydrated conditions is very heterogeneous in its backbone conformation (Shindo et al., 1980).

In contrast to DNA, the structures of RNA and DNA–RNA hybrids have been considered to be more or less a fixed form, either the A or A′ form (Milman et al., 1967; O'Brien & MacEvan, 1970). However, it has recently been found that DNA–RNA hybrids can occur in the B-like form under hydrated conditions: poly(rA)·poly(dT) is one example (Zimmerman & Pheiffer, 1981), and poly(rI)·poly(dC) is also so claimed (Arnott et al., 1983b).

In the present studies, we describe how to deduce the phosphodiester conformations from the ^{31}P NMR spectra of oriented fibers of various DNA and discuss the results in relation to the structural models determined from the X-ray fiber diffraction data and also to the single crystal structures of oligonucleotides.

Materials and Methods

Materials. Salmon sperm DNA (P-L Biochemicals) was purified by the standard phenol treatment. Lyophilized poly(rA)·poly(rU), poly(rA)·poly(dT), and poly(dA)·poly(dT) were also purchased from P-L Biochemicals, which were used for making fibers without further purification.

Fibers. Sodium salts of natural DNA fibers were prepared as before (Shindo et al., 1980). Each synthetic polymer was dissolved in a solution of 0.1 M NaCl and 0.1 mM EDTA (pH 7.4). After the solution was held overnight at about 4 °C, two volumes of cold ethanol were added, yielding a fibrous precipitate. The precipitate was collected by centrifugation, washed 3 times with 70% ethanol, and dried in a desiccator. A small amount of distilled water was added and held overnight, yielding a uniform viscous pellet. A sample was placed between the ends of a U-shaped piece of Chromel wire and left to dry, exposed to the atmosphere at about 4 °C. Homogeneous fibers of 3–5-mm length and 0.1–0.3-mm diameter were usually obtained. The fibers except for poly(rA)·poly(rU) exhibited a good extinction coefficient of polarized light. It

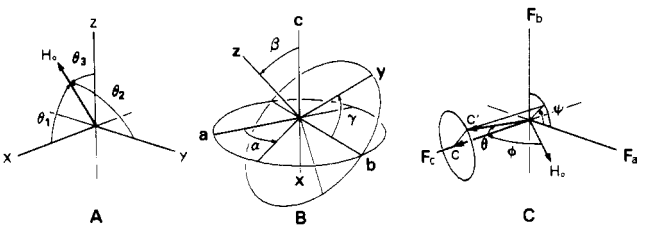

FIGURE 1: Coordinate systems. (A) Coordinate system (x, y, z) represents the principal axis system of the chemical shielding tensor and H_0 represents the static magnetic field. (B) Coordinate system (a, b, c) represents the molecular frame and axis c coincides with the helical axis of DNA as a reference frame. (C) Misalignment of a DNA molecule from the fiber axis F_c; vector **c** lies along fiber axis and **c′** represents the vector of the helical axis of misaligned DNA which makes an angle θ with respect to the fiber axis.

was difficult to form uniform fibers with Poly(rA)·poly(rU), and the fibers were turbid and very brittle probably because of the formation of polycrystals in the fiber.

NMR Measurements. Several fibers were aligned in parallel on a sample holder and held overnight for equilibration in the atmosphere of a given humidity before NMR measurements. Relative humidity was controlled by saturated solutions of various salts (O'Brien, 1948). The sample holder was inserted into a sample tube (6 mm o.d.) containing a piece of cotton moistened with the same saturated salt solution, and the sample tube was sealed and mounted on a goniometer. ^{31}P NMR spectra were measured at 80.7 MHz on a JNM-FX200 spectrometer (JEOL Co. Ltd.) equipped with an accessory of solid-state NMR unit. The measurements were performed at about 21 °C under cross-polarized and high proton decoupling conditions. The proton decoupling power was ca. 1.0 mT.

X-ray Diffraction. Several DNA samples were examined by X-ray fiber diffractions. Copper K_α radiation was obtained from a Norelco microcamera at room temperature. The humidity was controlled by continuously flushing the camera with a stream of helium which had been passed through an appropriate saturated salt solution. The X-ray exposure time was 3–6 h.

Computer Analysis. Model calculations were performed by using Fortran on a ACOS-6 (NEC Inc. Ltd.) at the Crystallographic Research Center of the Institute for Protein Research, Osaka University.

Theory

Spectral Analysis of Oriented DNA Fibers. Nall et al. (1981) and Shindo et al. (1980) have shown detailed analysis of ^{31}P NMR spectra from oriented DNA fibers, so we briefly describe its procedure below. Since chemical shift is a tensor quantity, an observed chemical shift of a nuclear spin in solids is written in terms of the direction cosines

$$\sigma^{obsd} = \sigma_{11} \cos^2 \theta_1 + \sigma_{22} \cos^2 \theta_2 + \sigma_{33} \cos^2 \theta_3 \quad (1)$$

where σ_{ii} values are the principal values of the chemical shielding tensor ($\sigma_{11} < \sigma_{22} < \sigma_{33}$). The direction cosine angles, θ_i, are the angles made between the principal axes of the tensor and the direction of the magnetic field as shown in Figure 1A. In case of oriented materials along one axis such as DNA fibers, it is convenient to define the molecular axis system (a, b, c) and to use Euler angles α, β, and γ instead of θ_1, θ_2, and θ_3 for the expression of a relative orientation of the axis systems. The behavior of the chemical shielding tensor is conveniently expressed by Wigner rotation matrices $D_{ab}^{(2)}(\Omega)$. When rotational transformations from the laboratory frame (magnetic field) to the principal axis system are carried out, namely

laboratory frame $\xrightarrow[\Omega(0,\phi,0)]{}$ fiber axis system $\xrightarrow[\Omega(\psi,\theta,0)]{}$ molecular axis system $\xrightarrow[\Omega(\alpha,\beta,\gamma)]{}$ principal axis system

then the observed chemical shift, $\sigma^{obsd}(\phi,\alpha)$, is given by [see, for example, Nall et al. (1981) and Mehring (1983)]

$$\rho_{20}^{lab} = \sqrt{\frac{3}{2}}\left(\sigma^{obsd} - \frac{1}{3}Tr\sigma_{ii}\right)$$

$$\rho_{20}^{lab} = \sum_{m,n,p} D_{p0}^{(2)}(0,\phi,0)D_{mp}^{(2)}(\psi,\theta,0)D_{nm}^{(2)}(\alpha,\beta,\gamma)\rho_{2n} \quad (2)$$

where $D_{mn}^{(2)}(\alpha,\beta,\gamma)$ is the Wigner rotation matrix of the second rank, ρ_{2n} is the irreducible coupling tensor of chemical shielding anisotropy, and the notations of the Euler angles correspond to those in Figure 1B,C. The principal axis system of the tensor is defined by Euler angles β and γ with respect to the molecular axis system (a, b, c). The fiber axis system is taken to be identical with the goniometer axis system (Figure 1C). The goniometer rotation angle ϕ between the fiber axis and the magnetic field direction can be chosen, and a series of the spectra, for example, the parallel ($\phi = 0°$) and the perpendicular ($\phi = 90°$) spectra, can be obtained. The second factor, $D_{mp}^{(2)}(\psi,\theta,0)$, in eq 2 takes into account the fact that molecules are not always perfectly aligned along the fiber axis. The population of misaligned molecules may be rapidly decreased as the tilt angle θ is increased, for which a Gaussian distribution may be assumed, and thus, the degree of the alignment may be represented by a standard deviation $\langle\theta\rangle$. A set of the spectra for a given tilt angle θ are calculated for all the possible values of Euler angles α and ψ with appropriate intervals and are weighted by a Gaussian function with a standard deviation $\langle\theta\rangle$. Finally, all sets of the spectra are summed up.

Euler angles β and γ are structurally dependent and may have intrinsic distributions. In case of the phosphodiesters of DNA, the principal axis system of the chemical shielding tensor of ^{31}P nuclei is reasonably related to the atomic coordinates of the phosphodiester (Kohler & Klein, 1976; Hertzfeld et al., 1978), so that the x axis is taken as the axis normal to the O–P–O plane, the y axis as the bisector of the vectors of two P–O bonds, and the z axis as normal to the above two axes. Thus, Euler angles β and γ can be, in principle, determined from the chemical shift spectra observed at two goniometer angles, and thus, the orientation of the phosphodiester relative to the molecular axis system can be estimated.

As is shown later, there are four important factors affecting spectral line shapes of DNA in solids: (1) imperfect alignments of DNA molecules along the fiber axis, (2) conformational multiplicity, i.e., distributions of Euler angles β and γ, (3) line broadening due to dipolar interactions, and (4) molecular motions. Item 1 is already included in eq 2 and item 2 is of much importance in the case of the B-form DNA having multiple conformations. Item 3 was first noticed by Nall et al. (1981), and its contribution to the line width was estimated to be about 1200 Hz; we found it to be about 400 Hz on the experimental basis (Shindo, 1984). Item 4 becomes important when DNA fiber is hydrated at high relative humidity. Because of the complicated motions in hydrated DNA, we will discuss this matter separately in the following paper (Fujiwara & Shindo, 1985).

Results

NaDNA Fibers. The ^{31}P NMR spectra of NaDNA fibers are shown in Figure 2 at various relative humidities. The spectra from the left to the right were obtained from the fibers oriented parallel, at 45°, and perpendicular to the magnetic field. NaDNA fiber is known to undergo a conformational transition from the A to the B form in the humidity range from 84% to 89% RH (Cooper et al., 1966). As is expected, rather drastic changes in the chemical shift and line shape can be seen in this humidity range. The A form of DNA fibers below this humidity range exhibits a typical spectral pattern for the axially oriented molecules with a single conformation: the parallel spectrum is a singlet, the 45° spectrum is a triplet, and the perpendicular spectrum is a bimodal pattern. In the transition region, the parallel spectrum shifts slightly upfield and becomes strikingly broadened, the central peak of the 45° spectrum is reduced in its intensity while that of the perpendicular spectrum becomes intensive. It is interesting to note that in this humidity range the separation between two peaks in the bimodal pattern of the A form remains unchanged but that its component is reduced with increasing relative humidity, suggesting that the interconversion between the A and B forms is slow compared with the NMR time scale. Furthermore, it should be noted that at about 84% RH the spectral span of the 45° spectrum is clearly narrower than that of the immobilized A form at 79% RH, although both the parallel and perpendicular spectra assigned to a part of the A form DNA remain unchanged. This observation indicates the occurrence of a small local conformational change, but we could not identify it with certainty.

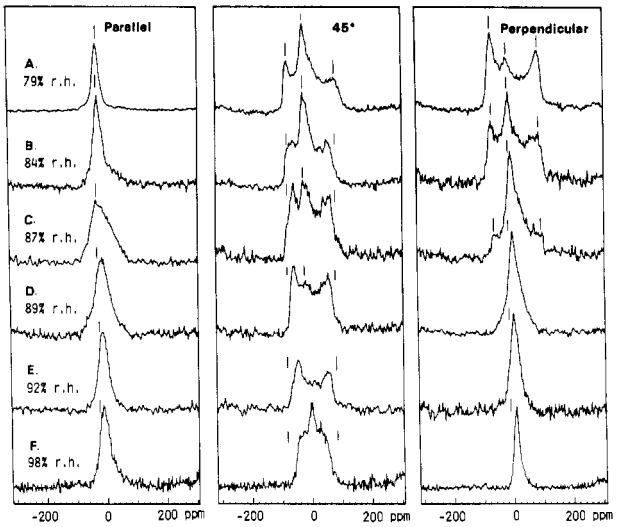

FIGURE 2: Proton dipolar decoupled ^{31}P NMR spectra (80 MHz) of salmon sperm NaDNA fibers as a function of relative humidity at different orientations of the fiber axis to the magnetic field as indicated. Relative humidity was controlled by saturated salt solutions: NH_4Cl for 79% RH, KBr for 84% RH, KCl for 87% RH, $ZnSO_4$ for 89% RH, sodium tartarate for 92% RH, and $KClO_3$ for 98% RH. Spectrometer conditions: spectral window 50 kHz; data points 2048 real; cross-polarization time 1.5 ms; delay time 2.5 s; line broadening 200 Hz; accumulation time 8–16 hs. Spectra F were measured by normal Fourier transform mode. Chemical shifts were measured as upfield positive relative to the phosphonic acid (85%).

At 89% RH the bimodal pattern characteristic of the A form DNA completely disappears as is seen in the perpendicular spectrum. The spectra of the B-form DNA can be characterized as follows: the parallel spectrum is a broad line shape of a Gaussian type, the 45° spectrum is a bimodal with a very weak peak at the center, and the perpendicular spectrum is a wedge-shaped line. With increasing relative humidity, the line width of the parallel spectrum becomes rapidly narrower but remains unchanged upon further increase in relative humidity. The bimodal pattern of the 45° spectrum at 98% RH becomes a bell-shaped pattern with a weak peak at about the center, and the perpendicular spectrum becomes continuously narrower and gradually shifts upfield. The behavior of the

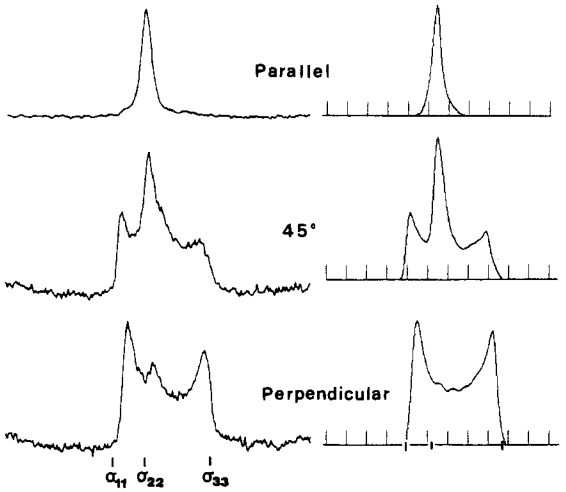

FIGURE 3: Observed and simulated ^{31}P NMR spectra for oriented fibers of the A-form DNA at goniometer angles between fiber direction and the magnetic field as indicated. The similated spectra have been calculated by using eq 2. See details in the text.

Table I: Observed Chemical Shifts and the Orientation Parameters of the Phosphodiesters of Polynucleotide Fibers at Various Relative Humidities

materials	RH (%)	chemical shifts (ppm) parallel	chemical shifts (ppm) perpendicular	Euler angles (deg) β	Euler angles (deg) γ
salmon	79	−25	−65, 92	71 ± 2	58 ± 3
NaDNA	92	−12	−1	(55 ± 5)	(30 ± 15)[a]
	98	−8	15		
poly(rA)·poly-	79	−28	−70, 98	75 ± 3	59 ± 5
(rU)	92	−26	−70, 95		
poly(rA)·poly-	79	−34	−63, 95	72 ± 3	48 ± 5
(dT)	95	−45, −20	11, 25		
poly(dA)·poly-	79	−9	−11		
(dT)	98	−12	−7		

[a] These Euler angles were estimated from line-shape analysis (Fujiwara & Shindo, 1985).

B-form DNA fibers such as the above mentioned was qualitatively interpreted in terms of the local fluctuation among the multiple conformations inherent to the B-form DNA and the rotational reorientation about the helical axis at high relative humidities (Shindo et al., 1984).

From the humidity dependence of ^{31}P NMR spectral patterns, it can be said that the immobilized form of NaDNA fibers is the A form. Figure 3 compares the observed spectra of NaDNA fibers at 79% RH with those calculated by using eq 2. By use of the observed principal values, $\sigma_{11} = -83$ ppm, $\sigma_{22} = -22$ ppm, and $\sigma_{33} = 110$ ppm (Terao et al., 1976; Shindo et al., 1980; Nall et al., 1981), the phosphodiester orientation represented by Euler angles β and γ was chosen so as to meet the chemical shifts of the peaks in the spectra from the fibers oriented parallel, at 45°, and perpendicular to the magnetic field. The line broadening in the simulated spectra was made by considering the imperfect alignment of the molecules with a standard deviation $\langle\theta\rangle = 12°$ and a 4 ppm width from other contributions. It is clear from Figure 3 that there is good agreement between the observed and the simulated spectra. The observed shift values and the determined Euler angles β and γ are listed in Table I. The values of β and γ are in good agreement with the results obtained for calf thymus DNA (Nall et al., 1981) and the A form of poly(dA-dT)·poly(dA-dT) (Shindo et al., 1981).

The B-form NaDNA is always observed at high relative humidities (89–98%). However, it is very difficult to predict

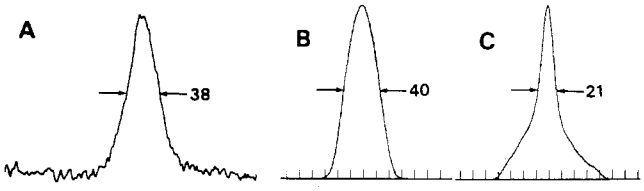

FIGURE 4: Observed (A) and simulated (B and C) ^{31}P NMR spectra for the B-form DNA fibers at 92% RH; the fiber axis is parallel to the magnetic field. Simulated spectrum B was calculated assuming distributions of the Euler angles β and γ, and spectrum C was calculated assuming a distribution of misalignment of DNA molecules from the fiber axis. The line widths at half-height are indicated in ppm.

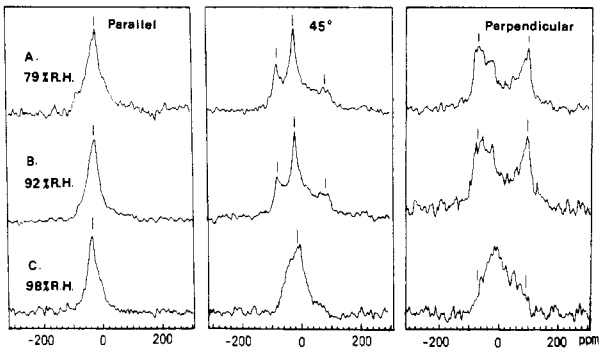

FIGURE 5: Proton dipolar decoupled ^{31}P NMR spectra (80.7 MHz) of poly(rA)·poly(rU) fibers as a function of relative humidity. Spectrometer conditions are almost the same as in Figure 2, except for accumulation time, 16–24 h.

the static geometry of the B form directly from the ^{31}P NMR spectra because of the existence of considerable molecular motions. In particular, a doublet of the 45° spectrum at 92% RH seems to be very unusual in view of the single lines in both parallel and perpendicular spectra. It is also remarkable that at 98% RH the total spectral line width decreases in the order of the spectra from the fibers oriented at 45°, parallel, and perpendicular to the magnetic field.

The observed parallel spectra under high humidity conditions were found to be usually broad compared with those of the A-form DNA fiber (line width 38–40 ppm at half-height of the parallel spectra at 92% and 98% RH in Figure 2), in spite of the fact that any motion must result in the motional narrowing of the spectral lines. The line shape of the parallel spectrum of NaDNA fibers at 92% RH is compared with those of calculated spectra. Out of several factors causing the line broadening, the contributions from the multiplicity in the backbone conformation and the imperfect alignment of the molecules within the fiber sample were found to be predominant (Shindo et all., 1980). When the effects of these factors were considered separately, spectrum B in Figure 4 was calculated by assuming Gaussian distributions of the Euler angles β and γ with standard deviations $\langle\beta\rangle = 5°$ and $\langle\gamma\rangle = 15°$. Spectrum C was calculated by assuming a Gaussian distribution of the molecular alignment with a standard deviation $\langle\theta\rangle = 20°$. It is clear from very distinctive line shapes between spectra B and C that the distribution term due to Euler angles can be fit much better to the observed spectrum A. Although the exact values of $\langle\beta\rangle$ and $\langle\gamma\rangle$ are rather arbitrary, it can clearly be stated that the distribution of the Euler angles is the most predominant factor that causes the line broadening of the spectra at high relative humidities.

Double-Stranded RNA, Poly(rA)·Poly(rU). As an example of double-stranded RNA, the ^{31}P NMR spectra from poly(rA)·poly(rU) fibers were measured at different relative humidities, and the results are shown in Figure 5. Not sur-

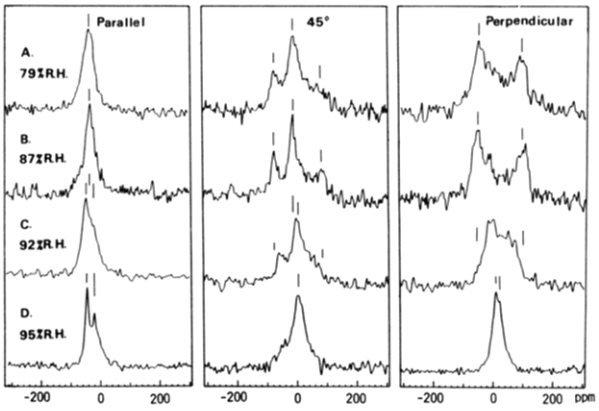

FIGURE 6: Proton dipolar decoupled ^{31}P NMR spectra (80.7 MHz) of poly(rA)·poly(dT) fibers as a function of relative humidity. Spectrometer conditions are almost the same as in Figure 5.

prisingly, the spectra display the typical fiber patterns very similar to those of the A form DNA. Computer simulation of the spectra at 92% RH yielded the best fitted Euler angles β and γ as listed in Table I. The fibers still retain their static spectral patterns up to 92% RH. Upon futher increase in humidity, both the perpendicular and the 45° spectra were collapsed into broad single lines, while the parallel spectrum becomes only slightly narrower but remains unaffected in its shift by hydration. This strongly suggests that the changes in shape are not due to conformational changes but due to the rotational motion about the helical axis. Thus, the results imply that the double-stranded RNA like poly(rA)·poly(rU), even with different base sequences on each strand, has an essentially identical backbone conformation and also that this polymer exhibits no conformational transition induced by hydration. Interestingly, the effect of molecular motions on the spectral patterns is different between NaDNA and RNA fibers: the total spectral span for poly(rA)·poly(rU) fibers at 98% RH decreases in the order of the spectra of the fibers oriented perpendicular, at 45°, and parallel to the magnetic field.

DNA–RNA Hybrid, Poly(rA)·Poly(dT). The ^{31}P NMR spectra from poly(rA)·poly(dT) fibers are shown in Figure 6 as a function of relative humidity. There is no change in the spectral patterns between 79% and 87% RH, which are very similar to those of the A-form DNA. Computer simulation yielded the best-fitted Euler angles β and γ as listed in Table I, together with the observed chemical shifts. Notably, the parallel spectrum at 95% RH displays resolved two peaks, clearly indicating that two distinct conformations exist in this polymer under hydrated conditions. Such resolved peaks can also be perceived, although not so clear, in the perpendicular spectrum. An asymmetric single line of the parallel spectrum at 92% RH reveals unresolved peaks, and therefore, a conformational transition appears to occur between 87% and 92% RH. The line narrowing and the changes in line shape of both the perpendicular and the 45° spectra in the high humidity range are considered to be the consequence of both the conformational changes and the rotational motion about the helical axis. The static geometry of this hybrid at high relative humidities can be determined only by the detailed line-shape analysis which takes into account the rotational motions, as is described in the following paper (Fujiwara & Shindo, 1985).

Poly(dA)·Poly(dT) Fibers. The samples that were commercially prepared so as to preserve the double-stranded form yielded well-oriented specimens as shown by the X-ray fiber diffraction (in Figure 7). On the basis of the Bragg reflections from the fiber at 79% RH, the axial spacing (31.4 Å) was

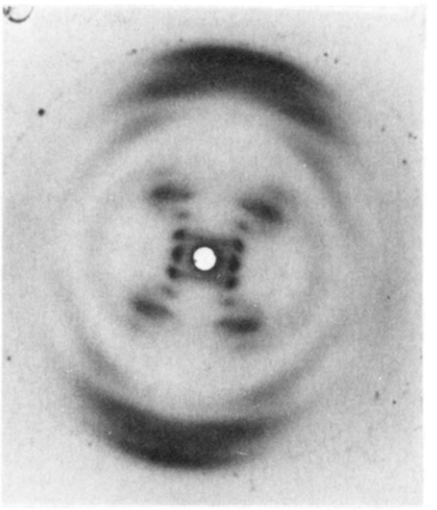

FIGURE 7: X-ray diffraction photograph of poly(dA)·poly(dT) fibers at 79% RH.

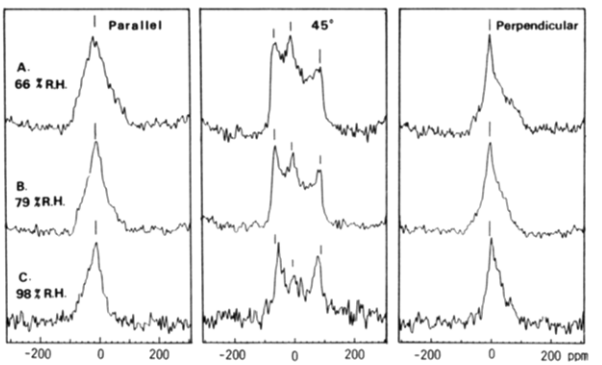

FIGURE 8: Proton dipolar decoupled ^{31}P NMR spectra (80.7 MHz) of poly(dA)·poly(dT) fibers as a function of relative humidity. Spectrometer conditions are almost the same as in Figure 2.

measured, corresponding to 9.6 residues per turn. The visual inspection of the diffraction pattern shows that the underlying intensity distribution is very similar to that observed for the crystalline form as α-B′ DNA by Arnott & Selsing (1974). Therefore, the poly(dA)·poly(dT) fibers used here can be referred to as the B′-form DNA (Arnott & Selsing, 1974). It is interesting to note that the axial spacing was continuously changed from 31.4 down to 25.5 Å with the decrease in the relative humidity from 98% to about zero RH, whereas the axial rise per residue was nearly constant (3.21–3.26 Å) in the same humidity range.

The ^{31}P solid-state NMR spectra from poly(dA)·poly(dT) fibers are shown in Figure 8. The strong dependence of the spectral pattern on the goniometer angle reveals that the molecules are well oriented along the fiber axis. At 66% RH where the molecules are presumably immobilized, the parallel spectrum is markedly broad (ca. 60 ppm in line width which may be compared to 25 ppm for the A-form DNA in Figure 2), and the perpendicular spectrum quite differs from the ordinary bimodal pattern such as that of the A-form DNA. Both the parallel and perpendicular spectra become narrow by hydration, but their peak positions remain almost unchanged. Three peaks can be seen in the 45° spectrum, of which the central peak is reduced in its intensity as the relative humidity increases. It is interesting to note that the two sets of spectra from poly(dA)·poly(dT) fibers at 79% and 98% RH very much resemble, in their patterns, the spectra of the B form of NaDNA fibers at 89% and 92% RH, respectively, indicating that the average phosphodiester orientation relative to the

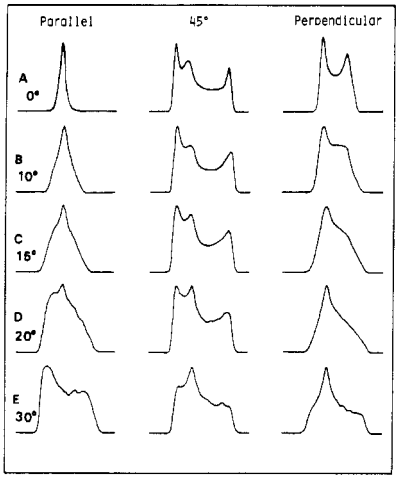

FIGURE 9: Calculated ^{31}P NMR spectra as a function of average tilt angle $\bar{\theta}$ for a structural model of DNA. The model is characterized by the structural parameters β and γ for the phosphodiester f the B-form DNA, i.e., Euler angles (β = 55° and γ = 30°), and by a tilt angle $\bar{\theta}$ of the helical axis from the fiber axis as indicated. A standard deviation $\langle\Delta\theta\rangle$ = 10° ffrom the average tilt $\bar{\theta}$ for molecular alignments was taken into account for all the spectra.

helical axis is nearly identical between poly(dA)·poly(dT) and NaDNA fibers under hydrated conditions.

As is seen in Figure 8, the parallel spectra of poly(dA)·poly(dT) are abnormally broad and rather like an inversed V-shape, for which two factors causing line broadening as illustrated in Figure 5 might give an interpretation. However, in view of the well-oriented specimens of this polymer having homogeneous sequenes, it is unlikely that the Gaussian distributions of the Euler angles β and γ and/or the imperfect molecular alignments give a reasonable interpretation. Alternatively, an interpretation for such abnormal line shapes may be rationalized by supposing that all DNA molecules and hence their helical axes tilt by a certain angle, $\bar{\theta}$ on the average, from the fiber axis. Figure 9 shows this situation. The spectra from left to right correspond to those for the fiber oriented parallel, at 45°, and perpendicular to the magnetic field. In view of the dependence of both the line shapes and line widths of the spectra on the tilt angle, $\bar{\theta}$, it seems clear that the observed spectra at 66% RH are most similar to those of the tilt angle between 15° and 20° and that the higher the humidity, the smaller the predicted tilt angle would be.

DISCUSSION

Earlier works on the X-ray fiber diffraction by Wilkins & co-workers (Langridge et al., 1960a,b; Fuller et al., 1965; Marvin et al., 1961) established the fundamental structures of naturally occurring DNA, which were designated the A, B, and C forms of DNA. Subsequently, several new conformational variants have been found for synthetic polynucleotides, and also, the extensive refinements of the structures of the canonical forms and new forms have been made with the aid of model buildings and/or theoretical calculations, in order to fit the models to their X-ray diffraction patterns. Such refinements for individual forms have been carried out by assuming a single or two conformations with the helical symmetry. However, these structural models dictated by X-ray fiber diffraction data are not necessarily unique. Therefore, it is particularly important to test these proposed models by a method other than X-ray diffraction.

Recently, X-ray single crystal structures of several oligonucleotides have become available (Wing et al., 1980; Dickerson et al., 1982; Wang et al., 1979, 1982, 1983). By use of

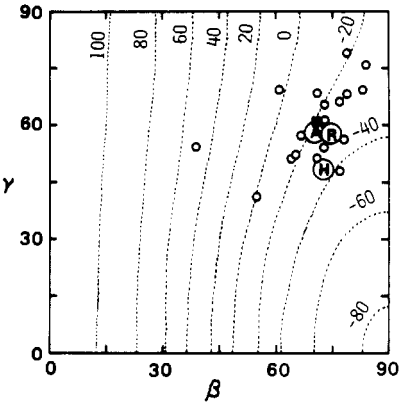

FIGURE 10: Plots of the Euler angles β and γ for the individual phosphodiesters of a decamer, r(GCG)d(TATACGC). The Euler angles represent the orientations of the principal axis system of the chemical shift tensor relative to the molecular frame (see Figure 1B). Plots A, R, and H represent the Euler angles estimated for the A or A′ form of salmon sperm DNA, poly(rA)·poly(rU) and poly(rA)·poly(dT) fibers, respectively. A rectangular plot represents an averaged value over all the plots from the decamer. Dotted lines are the contour lines of the chemical shift values in ppm when the fiber oriented parallel to the magnetic field.

their atomic coordinates, the ^{31}P NMR spectra can be predicted for the hypothetical DNA fibers that are composed of the repeating units of such oligomers. Comparison of these results with the NMR data from various DNA fibers may be helpful in understanding the underlying features of the structure of DNA.

Distribution of the Phosphodiester Conformations of Oligonucleotides. The X-ray single crystal studies on various oligonucleotides are now extensively in progress. It is worthwhile to calculate the phosphodiester orientation of each residue with respect to the helical axis of the oligomer and to compare it with the Euler angles β and γ from the ^{31}P NMR experiments on DNA fibers.

Most of the oligonucleotides tend to form the single crystals of the A-like DNA, but the B DNA in rare cases, probably because the A-form DNA may be favorable for the molecular packing in crystals. We chose a decamer, r(GCG)d(TATACGC), as a typical A form which consists of blocks of DNA and DNA–RNA hybrid in the duplex (Wang et al., 1983), although there are other single crystal structures available for the A-form DNA (Wang et al., 1982). We did not choose them because the definition of the helical axis is somewhat ambiguous for such short oligomers. By use of the atomic coordinates of the phosphodiesters in the decamer and its defined helical axis (S. Fujii, private communications), the Euler angles of each phosphodiester orientation relative to the helical axis were calculated and the results are plotted in Figure 10. Plots A, H, and R in this figure represent the Euler angles experimentally determined from the ^{31}P NMR spectra of the A or A′ form of NaDNA, poly(rA)·poly(dT), and poly(rA)·poly(rU) fibers, respectively. The latter two polymers are known to form the A′ conformation (Zimmerman & Pheiffer, 1981; Arnott et al., 1972). The solid rectangular plot corresponds to the average of Eular angle over all the plots from the decamer.

Two very interesting points can be noted from Figure 10: first, most plots are clustered together in a rather narrow area, namely, within about ±7° in Euler angles, and second, the Euler angles obtained from the NMR data of the A and A′ forms are within the same cluster. There are a few exceptions in that the two plots located slightly away from the cluster are due to deoxyribose moieties at position 8 on one strand and position 9 on the other strand in the r(GCG)d(TA-

Table II: Backbone Conformations (Dihedral Angles) of the Structural Models Proposed for the B and A Forms of DNA and Polynucleotides and Chemical Shifts of the Parallel Spectra Calculated for the Models

materials	no.	strands	P–O5′ α	O5′–C5′ β	C5′–C4′ γ	C4′–C3′ δ	C3′–O3′ ϵ	O3′–P ξ	σ (ppm)	references
poly(dA-dT)·	1	dApdT	−60			110		−60	−29.5	Klug et al. (1979)
poly(dA-dT)	2	dTpdA	−50			155		−120	2.5	
	3	dApdT	−45	142	55	142	−157	−145	16.0	Arnott et al. (1983a)
	4	dTpdA	−72	142	69	154	−133	−153	49.3	
poly(dA)·poly(dT)	5	dApdA	−60	172	54	81	−170	−59	−48.5	Arnott et al. (1983b)
	6	dTpdT	−41	186	43	152	−171	−121	−32.3	
poly(rA)·poly(dT)	7	rAprA	−88	174	75	97	−146	−77	−47.5	Zimmerman & Pheiffer (1981)
at 98% RH	8	dTpdT	−180	96	166	152	−176	−36	−27.0	
B-form DNA	9		−41	136	38	139	−133	−157	–[a]	Arnott et al. (1983b)
	10		−31	149	37	132	−157	−134	−18.0	Premilat & Albiser (1983)
	11		−60	180	57	122	−187	−91	−33.5	Levitt (1978)
A-form DNA	12		−50	172	42	79	−145	−78	−16.0	Arnott et al. (1983b)
	13		−60	164	51	81	−136	−87	−13.3	Premilat & Albiser (1983)
α-A RNA	14		−62	180	48	83	−151	−74	−6.0	Arnott & Hukins (1972)
α-A′ RNA	15		−65	193	44	83	−168	−60	−17.5	Arnott & Hukins (1972)

[a] Atomic coordinates of the structure were not available.

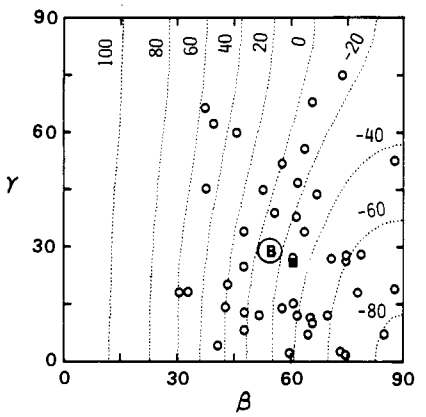

FIGURE 11: Plots of the Euler angles β and γ for the individual phosphodiesters of two dodecamers, d(CGCGAATTCGCG) and its derivative d(CGCGAATTbr^{5}CGCG). Plot B represents the Euler angles observed for the B form of salmon sperm DNA fibers at 92% RH. Other symbols are the same as in Figure 10.

TACGC) duplex. Nevertheless, the results discussed above strongly support the idea that the phosphodiesters belonging to the A family are restricted in their conformations, and thus, the backbone conformations are very much similar to each other.

Oligonucleotides, d(CGCGAATTCGCG), and its derivative d(CGCGAATTbr^{5}CGCG) are the only oligomers found to be ascribed to the canonical B form of DNA (Fratini et al., 1982). Figure 11 shows a distribution pattern of the Euler angles calculated for all the phosphodiesters in the single crystals of the above two dodecamers. Strikingly, the Euler angles are significantly widely scattered over the ranges from 30° to 90° and from 0° to 70° for β and γ, respectively. The distribution patterns of the Euler angles were very much similar to each other between the two dodecamers, although the bending angles of their helical axis are quite different: 19° for the mother oligomer and about 0° for its derivative (Fratini et al., 1982). Plot B represents the Euler angles estimated from the computer simulation of the spectra of NaDNA fibers at 92% and 98% RH and the solid rectangular plot represents the average values for the two dodecamers. Interestingly, plot B is very close to the average of the Euler angles. As we previously showed (Shindo et al., 1984), the lithium salt of DNA fibers at 66% RH has been ascribed to the immobilized B form, for which the distribution of the Euler angles was found to be quite similar to that for the single crystals of the dodecamers, indicating that the backbone conformation of the B-form DNA is indeed very heterogeneous, more so than we estimated previously (Shindo et al., 1980).

Synthetic Polynucleotides. The lack of sequence heterogeneity in repeating sequence polynucleotides led to a marked enhancement of the resolution obtainable in the structural studies, as compared to the studies with native DNA. In fact, the NMR study with alternating sequence poly(dA-dT) fibers revealed the general features of the structure of DNA; that is, the A form had a single backbone conformation while the B form had two distinct conformations (Shindo & Zimmerman, 1980). This polymer exhibited a sharp single line in the parallel spectrum at low RH while it exhibited two resolved peaks at high RH indicating that it has an alternating backbone conformation on each strand under highly hydrated conditions. Similarly, the hybrid poly(rA)·poly(dT) fibers ascribed to the A′ form at low RH exhibited a single line in the parallel spectrum, while the hydrated form of the hybrid exhibited a doublet. In this case, however, two distinct conformations can be tentatively ascribed to the antiparallel chains with different conformations (Shindo & Matsumoto, 1984). There are two plausible reasons why the hydrated form has two distinct conformations: one is the difference in the sugar moiety on the two strands, and the other is the difference in the base sequences. As shown in the ^{31}P NMR spectra from the poly(rA)·poly(rU) (Figure 5) and the poly(dA)·poly(dT) fibers (Figure 8), the former RNA undergoes no conformational transition and retains the conformation of the A family at any humidity, nor does the latter DNA exhibit any drastic conformational change but retains the conformation of the B family. As for the two peaks in the parallel spectrum from the hybrid poly(rA)·poly(dT) fibers at 95% RH (Figure 6), the downfield peak assigned to the poly(rA) strand is much sharper than the upfield peak assigned to the poly(dT) strand (Shindo & Matsumoto, 1984), indicating that the conformation of the poly(rA) strand is restricted while the poly(dT) strand has more freedom to vary its conformation. Therefore, it is most likely that the bimorphic structure observed for the poly(rA)·poly(dT) fibers is not due to the difference in base sequences on the two strands but rather due to the difference in sugar moiety. This has an important implication in that such a bimorphic structure may be a general feature of DNA–RNA hybrids under highly hydrated conditions.

One of the purposes in the present study is to test the structural models proposed for various synthetic DNA fibers. The conformational parameters reported on their models are collected in Table II. The procedures for the tests were performed in the same manner as done for oligonucleotides. By use of the atomic coordinates of the structural models proposed for various polynucleotide duplexes, the phosphodiester orientation relative to the helical axis as described by

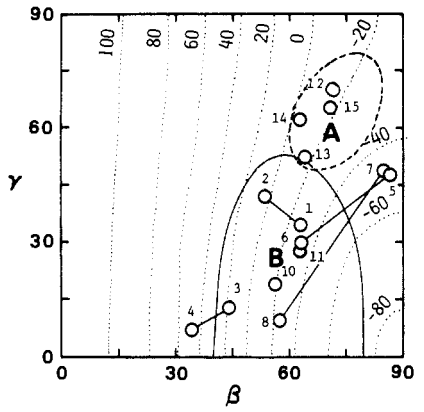

FIGURE 12: Plots of the Euler angles β and γ calculated from the atomic coordinates of the phosphodiesters of the structural models which have been determined from X-ray fiber diffractions of DNA and various polynucleotides. Numbers in the figure coincide with material numbers in Table II. Area A corresponds to the structure of the A family of DNA and area B to that of the B family of DNA.

Euler angles β and γ was calculated, and they are plotted in Figure 12. In this figure, the inside area surrounded by the solid line is regarded as the most probable Euler angles which the phosphodiesters in the B-form DNA can take. The line is drawn in such a way that the area includes both the distribution width of the Euler angles estimated from the observed spectra of NaDNA fibers at 89% RH and about three-fourths of the total 44 plots for the dodecamers in Figure 11. Similarly, the broken line is considered to be the most probable Euler angles for the phosphodiesters of the A and A′ forms.

Two structural models were proposed for an alternating sequence, poly(dA-dT)·poly(dA-dT). Plots 1 and 2 correspond to the model proposed by Klug et al. (1979) and plot 3 and 4 to that proposed by Arnott et al. (1983a). As was stated by Klug et al. (1979) and also as is seen in Table II, the sequences dApdT and dTpdA in the former model are quite different in dihedral angles δ and ξ; the conformation of the former is similar to that of the A family of DNA, while the latter is similar to the B-form DNA of Levitt (1978). On the other hand, in the model of Arnott et al. (1983a) the conformations of the two sequences dApdT and dTpdA are slightly different in dihedral angles α and ϵ, but both are essentially similar to the B form of Arnott et al. (1983a). As we previously reported, this alternating sequence DNA was found to exhibit two resolved peaks at −27 and 3 ppm in the parallel spectrum at 98% RH (Shindo & Zimmerman, 1980). The model of Klug et al. (1979) yielded −29 and 2.5 ppm as the corresponding shift values, which are in excellent agreement with the observed values (−27 and 3 ppm). The model of Arnott et al. (1983a), however, led to too high shift values (16 and 49 ppm).

Zimmerman & Pheiffer (1981) have proposed a B-like structure for the hydrated form of the poly(rA)·poly(dT) hybrid, which was the first example revealing that the duplex with different sequences has different conformations on two strands. As can be seen in Table II, the poly(rA) strand has a conformation similar to that of the A form, whereas the poly(dT) strand has quite different dihedral angles α, β, and γ; i.e., a conformation (t,g,t) vs. a standard conformation (g^-,t,g). The shift values calculated for this model are −45.7 and −27.0 ppm for the poly(rA) and poly(dT) strands, respectively. These values are in excellent agreement with the observed values (−45 and −20 ppm). As is described in the following paper (Fujiwara & Shindo, 1985), the model receives further support in that the spectral patterns at 92% RH in Figure 6 are given by the sum of the spectra from the A-form strand and the B-form strand; this is consistent with the fact that plot 7 lies close to the A area and that plot 8 is at the center of the B area in Figure 12.

Arnott et al. (1983a) recently suggested the general idea that DNA and DNA–RNA hybrids with different sequences have different conformations on two strands, and they reported a bimorphic structure for poly(dA)·poly(dT) as one of the examples. The shift values of the parallel spectrum calculated for this model are −49 and −32 ppm, which do not agree with the shift value (−12 ppm) observed for this fiber at 98% RH (Table I). A broad line width (ca. 60 ppm) of the parallel spectrum indicates that poly(dA)·poly(dT) fibers might have a bimorphic structure, but the average of Euler angles of the phosphodiesters on two strands should be in the B area in Figure 12. The same spectral patterns were also observed for poly(dT)·poly(dC) fibers (data not shown). We are not certain why the spectral lines are so broad in spite of the fact that this polymer is composed of homogeneous base sequences and that the fibers were of a well-oriented specimen. We noted under Results that the helical axis might tilt by 15–20° with respect to the fiber axis, indicating that this type of DNA might have a coiled double helix in a regular fashion. It is interesting to note that the apparent angle between the base pair and the helical axis decreases as the DNA is stretched by an electric field (Lee & Charney, 1982; Diekman et al., 1982), suggesting that DNA might be supercoiled under normal conditions (Lee & Charney, 1982). It was also demonstrated by the computer simulation of molecular dynamics (Levitt, 1983) that a high degree of conformational flexibility was available to DNA and that smooth bending motion was a normal mode of the global motions of DNA, which was remarkable for the $(dA)_{24}\cdot(dT)_{24}$ sequence. The coiled double helix predicted here for poly(dA)·poly(dT) fibers may be consistent with these findings. Furthermore, the humidity dependence of the axial spacing determined from X-ray fiber diffractions is likely to correlate to such a tilt angle. Yet, we anticipate a detailed X-ray diffraction study on poly(dA)·poly(dT) fibers as a function of relative humidity.

CONCLUSIONS

The ^{31}P solid-state NMR method used here is concerned only with information on the phosphodiester orientations of DNA. Therefore, the ^{31}P NMR data from DNA fibers do not provide direct information about the helical parameters such as the pitch and axial rise per residue. However, fortunately, the backbone conformations for the A-form DNA characterized by the dihedral angles of successive six bonds are likely to be restricted to a limited range. That is why all the models proposed for the A family of DNA and RNA are consistent with our ^{31}P NMR data (Figure 12).

The ^{31}P NMR method is extremely useful to elucidate the backbone conformations of DNA, especially under highly hydrated conditions where the X-ray fiber diffraction method cannot tell much about structural details such as multiplicity of the backbone conformations. The presence of multiple conformations in the B form of DNA fibers was shown to be an intrinsic nature of the B form DNA with random sequences; this seems to correlate with the fact that the conformations proposed for the B-form DNA differ from one investigator to another (Table II). The models proposed by Arnott et al. (1983b) and Premilate & Albiser (1983) are more or less similar to each other but different from that of Levitt (1978) in dihedral angles, α, β, γ, ϵ, and ξ. Both models (Levitt, 1978; Premilat & Albiser, 1983) seem to give a good fit to our NMR data of the B-form DNA. Therefore, it cannot be determined which conformer represents the B-form DNA; this is in ac-

cordance with the conformational flexibility of the B-form DNA (Levitt, 1978, 1983). As we previously noted (Shindo et al., 1980, 1984), the backbone conformation of the B-form DNA is very heterogeneous, and each segment of the backbone may have a time-averaged conformation under highly hydrated conditions. We, therefore, believe that the sequence dependence of the secondary structure of the B-form DNA is a reflection of statistic populations among many conformations allowed for particular sequences.

ACKNOWLEDGMENTS

We thank Dr. S. Fujii of Osaka University for providing us with the atomic coordinates of the single crystal structure of an oligonucleotide, r(GCG)d(TATACGC), and Dr. M. Levitt of Wisemann Institute in Israel for providing us with the atomic coordinates of the structure of the B-form DNA determined by energy minimization. We also greatly appreciate Dr. S. B. Zimmerman of the National Institutes of Health for measuring X-ray diffractions of poly(dA)·poly(dT) fibers.

Registry No. Poly(rA)·poly(rU), 24936-38-7; poly(rA)·poly(dT), 27156-07-6; poly(dA)·poly(dT), 24939-09-1; r(GCG)d(TATACGC), 80804-89-3; d(CGCGAATTCGCG), 77889-82-8; d(CGCGAATTbr^{5}CGCG), 83661-70-5.

REFERENCES

Arnott, S., & Selsing, E. (1974) *J. Mol. Biol. 88*, 509–521.

Arnott, S., Hukins, D. W. L., & Dover, S. D. (1972) *Biochem. Biophs. Res. Commun. 48*, 1392–1399.

Arnott, S., Chandrasekaran, R., Hall, I. H., & Puigjaner, L. C. (1983a) *Nucleic Acids Res. 11*, 4141–4155.

Arnott, S., Chandrasekaran, R., Puigjaner, L. C., Walker, J. K., Hall, I. H., & Birdsall, D. L. (1983b) *Nucleic Acids Res. 11*, 1457–1474.

Cohen, J. S., Wooten, J. B., & Chatterjee, C. L. (1981) *Biochemistry 20*, 3049–3055.

Cooper, P. J., & Hamilton, L. D. (1966) *J. Mol. Biol. 16*, 562–563.

Dickerson, R. E., Kapka, M. L., & Drew, H. R. (1982) in *Structure and Dynamics: Nucleic Acids and Proteins* (Clementi, E., & Barma, R. H., Eds.) pp 227–257, Academic Press, New York.

Diekmann, S., Willen, W., Morgneyer, B., Wells, R. D., & Porschke, (1982) *Biophys. Chem. 15*, 157–167.

Drew, H. R., Wing, R. M., Takano, T., Broka, C., Tanaka, S., Itakura, K., & Dickerson, R. E. (1981) *Proc. Natl. Acad. Sci. U.S.A. 78*, 2179–2183.

Eckstein, F., & Jovin, T. M. (1983) *Biochemistry 22*, 4546–4550.

Fujiwara, T., & Shindo, H. (1985) *Biochemistry* (following paper in this issue).

Fuller, W., Wilkins, M. H. F., Wilson, H. R., & Hamilton, L. D. (1965) *J. Mol. Biol. 12*, 60–76.

Fratini, A. V., Kapka, M. L., Drew, H. R., & Dickerson, R. E. (1982) *J. Biol. Chem. 257*, 14686–14707.

Herzfeld, J., Griffin, R. G., & Harberkorn, R. A. (1978) *Biochemistry 17*, 2711–2718.

Klug, A., Jack, A., Viswamitra, M. A., Kennard, O., Shakked, Z., & Steitz, T. A. (1979) *J. Mol. Biol. 131*, 669–680.

Kohler, S. J., & Klein, M. P. (1976) *Biochemistry 15*, 967–973.

Langridge, R., Wilson, H. R., Hooper, C. W., Wilkins, M. H. F., & Hamilton, L. D. (1960a) *J. Mol. Biol. 2*, 19–37.

Langridge, R., Marvin, D. A., Seeds, W. E., Wilson, H. R., Hooper, C. W., Wilkins, M. H. F., & Hamilton, L. D. (1960b) *J. Mol. Biol. 2*, 38–64.

Lee, C.-H., & Charney, E. (1982) *J. Mol. Biol. 161*, 289–302.

Leslie, A. G. W., Arnott, S., Chandrasekaran, R., & Ratliff, R. L. (1980) *J. Mol. Biol. 143*, 49–72.

Levitt, M. (1978) *Proc. Natl. Acad. Sci. U.S.A. 75*, 640–644.

Levitt, M. (1983) *Cold Spring Harbor Symp. Quant. Biol. 27*, 251–262.

Marvin, D. A., Spencer, M., Wilkins, M. H. F., & Hamilton, L. D. (1961) *J. Mol. Biol. 3*, 547–565.

McIntosh, L. P., Grieger, I., Eckstein, F., Zarling, D. A., van der Sande, J. H., & Jovin, T. M. (1983) *Nature (London) 304*, 83–86.

Mehring, M. (1983) in *Principles of High Resolution NMR in Solids*, 2nd revised ed., Springer-Verlag, Berlin, Heidelberg, New York.

Milman, G., Langrige, R., & Chamberlin, M. J. (1967) *Proc. Natl. Acad. Sci. U.S.A. 57*, 1804–1810.

Nall, B. T., Rothwell, W. P., Waugh, J. S., & Rupprecht, A. (1981) *Biochemistry 20*, 1881–1887.

O'Brien, F. E. M. (1948) *J. Sci. Instrum. 25*, 73–76.

O'Brien, E. J., & MacEvan, A. (1970) *J. Mol. Biol. 48*, 243–261.

Patel, D. J., Canuel, L. L., & Pohl, F. M. (1976) *Proc. Natl. Acad. Sci. U.S.A. 76*, 2508–2511.

Premilat, S., & Albiser, G. (1983) *Nucleic Acids Res. 11*, 1897–1908.

Shindo, H. (1984) in *Phosphorus-31 NMR* (Gorenstein, D., Ed.) pp 401–422, Academic Press, New York.

Shindo, H., & Zimmerman, S. B. (1980) *Nature (London) 283*, 690–691.

Shindo, H., & Matsumoto, U. (1984) *J. Biol. Chem. 259*, 8682–8684.

Shindo, H., Simpson, R. T., & Cohen, J. S. (1979) *J. Biol. Chem. 254*, 8125–8128.

Shindo, H., Wooten, J. B., Pheiffer, B. H., & Zimmerman, S. B. (1980) *Biochemistry 19*, 518–526.

Shindo, H., Wooten, J. B., & Zimmerman, S. B. (1981) *Biochemistry 20*, 745–750.

Shindo, H., Fujiwara, T., Akutsu, H., Matsumoto, U., & Shimidzu, M. (1984) *J. Mol. Biol. 174*, 221–229.

Terao, T., Matsui, S., & Akasaka, K. (1977) *J. Am. Chem. Soc. 99*, 6136–6138.

Wang, A. H.-J., Quigley, G. J., Kolpok, F. J., Grawford, J. L., van Boom, J. H., van der Marel, G., & Rich, A. (1979) *Nature (London) 282*, 680–686.

Wang, A. H.-J., Fujii, S., van Boom, J. H., & Rich, A. (1982) *Proc. Natl. Acad. Sci. U.S.A. 79*, 3968–3972.

Wang, A. H.-J., Fujii, S., van Boom, J. H., van der Marel, G. A., van Boeckel, S. A. A., & Rich, A. (1983) *Nature (London) 299*, 601–604.

Wing, R., Drew, H., Takano, T., Broka, C., Tanaka, S., Itakura, K., & Dickerson, R. E. (1980) *Nature (London) 287*, 755–758.

Zimmerman, S. B. (1982) *Annu. Rev. Biochem. 51*, 390–426.

Zimmerman, S. B., & Pheiffer, B. H. (1981) *Proc. Natl. Acad. Sci. U.S.A. 78*, 78–82.